Available online at www.eccomasproceedia.org
Eccomas Proceedia COMPDYN (2025) 949-960

ECCOMAS
Proceedia

COMPDYN 2025
10th ECCOMAS Thematic Conference on
Computational Methods in Structural Dynamics and Earthquake Engineering
M. Papadrakakis, M. Fragiadakis (eds.)
Rhodes Island, Greece, 15-18 June 2025

IMPACT OF MASONRY INFILLS ON THE NONLINEAR SEISMIC RESPONSE OF IRREGULAR RC BUILDINGS

M. Ferraioli[1], A. Lavino[1], O. Pecorari[1], and S. Mottola[1]

[1] Department of Engineering, University of Campania "Luigi Vanvitelli", Aversa, Italy
{massimiliano.ferraioli, angelo.lavino, Osvaldo.pecorari, salvatore.mottola}@unicampania.it

Abstract

Despite significant research efforts, understanding the seismic behavior of infilled reinforced concrete (RC) buildings remains challenging due to the complex interaction between infill walls and the structural frame, along with various influencing factors. Current seismic codes generally classify infill walls as non-structural elements, and standardized guidelines for their modeling and analysis are still lacking. However, completely disregarding their impact may not be conservative, as infill masonry walls can significantly influence seismic performance. Recognizing this effect, Eurocode 8 mandates an amplification of seismic action effects in certain cases of infill irregularity. This study assesses the adequacy of these design provisions by examining various in-plan layouts of infill walls that fall within the code's limits, where action effect amplification or additional countermeasures are not explicitly required. Nonlinear static and dynamic analyses were performed, accounting for masonry cracking, crushing, and the deterioration of both stiffness and strength. The findings highlight that neglecting the role of infills may not always be safe. In specific cases analyzed, torsional effects and soft-story mechanisms led to structural failure, despite Eurocode 8 not mandating action effect amplification. Moreover, the results suggest that the additional shear demand induced by masonry infills, although minimal, can still contribute to an increased vulnerability of RC buildings.

Keywords: Infill masonry walls, Seismic response, Nonlinear analysis.

ISSN:2623-3347 Published by Eccomas Proceedia.
Peer-review under responsibility of the organizing committee of COMPDYN 2025.
doi: 10.7712/120125.12461.26397

1 INTRODUCTION

Masonry-infilled reinforced concrete (RC) frames are commonly used in low- to mid-rise buildings, including those in seismic-prone areas. Unreinforced masonry infill walls are preferred for interior and exterior partitions due to their cost-effectiveness, durability, and insulation properties. However, past earthquakes have revealed that infill walls significantly influence a building's seismic performance. Damage assessments show that irregularly distributed infill walls can alter structural responses, leading to failure mechanisms that require further study. In masonry panels are often built in direct contact with RC frames, enhancing overall structural stiffness. However, their brittle nature and high initial stiffness can be detrimental under earthquake loading. Uneven distribution of infill walls, combined with material degradation under cyclic loading, may cause irregularities in plan and elevation. One critical issue is the "soft-story" effect, where an open ground floor—typically for commercial use—makes the structure vulnerable to collapse [1-2]. Similarly, irregular infill distribution in plan can induce torsional effects, increasing deformation demands in certain areas [3-4]. While infill walls improve strength and stiffness, they may also introduce unintended seismic vulnerabilities. Their stiffness changes the building's natural frequency, influencing seismic demand. Acting as diagonal struts, infills generate additional forces in beams and columns, raising shear demands at beam-column joints, which can lead to brittle failures. Buildings without proper seismic design are especially at risk of soft-story collapse, short-column effects, and torsional instability. Research on the seismic behavior of infilled RC frames dates back to the 1950s, with experimental studies examining frame-infill interactions and numerical models ranging from simplified strut approaches to advanced finite element simulations [5-9]. However, accurately predicting these interactions remains a challenge due to the complex, nonlinear properties of masonry and concrete. Variability in experimental data and multiple factors influencing infill performance make it difficult to establish universal design standards. Critical factors affecting failure mechanisms include the type of infill, construction method, aspect ratio, openings in masonry panels, column-to-beam stiffness ratios, and axial loads on columns. Despite extensive research, gaps remain in developing reliable models and guidelines for incorporating infill effects into seismic assessments.

2 MASONRY INFILLS IN SEISMIC CODES

In conventional building design, masonry infill panels are typically regarded as non-structural elements, meaning their influence on structural behavior is often disregarded in both analysis models and design procedures. As a result, the actual seismic performance of a structure can significantly deviate from predictions, particularly under strong ground motions. The complexity of frame-infill interaction has led to significant differences in design approaches across various countries. Many seismic codes provide only general recommendations for non-structural elements without explicitly addressing the impact of infill panels on seismic behavior. For instance, Eurocode 8 [10] does not require masonry infills to be explicitly considered structural components, leading to their exclusion in standard analyses. While the code aims to mitigate the negative effects associated with infill walls, it also neglects their potential benefits. Specifically, Eurocode 8 [10] accounts for plan irregularities by increasing the accidental eccentricity factor twofold. Regarding vertical irregularities, uniformly distributed infills can help decrease deformation demands and enhance energy dissipation capacity. Conversely, irregular distributions may increase seismic-induced deformation and trigger brittle failure mechanisms, such as torsional effects and soft-story collapses. In cases where infills are uniformly distributed, their overall stiffening and strengthening effects can be conservatively ignored, provided that any increase in seismic force demand is offset by enhanced strength due

to the infills. However, localized shear effects on RC members must still be considered. Additionally, non-apparent soft-story effects—where failure of infills in a specific story leads to weak-story behavior—can be neglected in regularly infilled frames, as lateral drift demands are typically concentrated in lower stories and remain below critical thresholds for instability [11]. For irregular infill distributions in elevation, seismic forces should be amplified using a magnification factor. The Italian Code [12-13] recommends a fixed amplification factor of 1.40 for potentially weak stories, while Eurocode 8 [10] provides a variable magnification factor (K_{IR}) based on the reduction in lateral resistance of masonry infills relative to adjacent stories and the overall seismic demand:

$$K_{IR} = \left(1 + \frac{\Delta V_{Rw}}{\Sigma V_{Ed}}\right) \leq q \tag{1}$$

where ΔV_{Rw} represents the total reduction in lateral resistance of the masonry infill walls in the specified story, relative to the more infilled story above; ΔV_{Ed} is the sum of the seismic shear forces acting on all structural vertical elements of the story concerned, q is the behavior factor. In contrast, U.S. codes, such as FEMA 356 [14], suggest macro-modeling approaches where masonry infills are represented as equivalent diagonal compression struts with properties derived from empirical relationships, such as those proposed by Mainstone [15].

3 MODELING AND VALIDATION

3.1 Background

The interaction between masonry infill and RC frame results in highly nonlinear inelastic behavior influenced by several factors: cracking and yielding in the bare frame (including bond-slip effects), stiffness degradation and crushing in the masonry infills, and variations in the panel-frame interface, such as changes in contact length and bond-friction mechanisms. Mainstone [15] provided an empirical equation, based on both experimental and analytical data, to determine the equivalent strut width:

$$\frac{w}{d} = 0.175 \cdot \lambda_n^{-0.4} \tag{2}$$

where d represents the diagonal length of the masonry panel and λ_n is the relative panel-to-frame stiffness. This formulation became widely recognized and was later adopted in FEMA-274 [16] and FEMA-306 [17]. Subsequent studies explored more advanced models to improve the prediction of frame-infill interaction effects. These methods are broadly categorized into micro-modeling and macro-modeling approaches. Micro-modeling, primarily based on the Finite Element Method (FEM), requires detailed modeling of individual masonry blocks, mortar joints, and interface elements to simulate shear sliding. Macro-modeling, on the other hand, represents the infill as an equivalent diagonal strut, offering a simpler and more computationally efficient method, though it cannot capture local effects. Asteris *et al.* [18] and Crisafulli *et al.* [19] conducted extensive literature reviews on these modeling techniques. Crisafulli *et al.* [20] introduced a simplified macro-model consisting of two pairs of diagonal struts for axial load transfer and two pairs of shear struts to simulate shear transmission within the panel. Cavaleri *et al.* [21] further refined force-displacement relationships by incorporating results from experimental testing to improve accuracy in cyclic and monotonic loading conditions.

3.2 Hysteretic Model Calibration

In this study, the masonry infills were modeled using the macro-model developed by Crisafulli *et al.* [20], which represents the infill panel with two parallel diagonal struts in each direction to carry axial loads, along with a shear strut responsible for transmitting shear forces from the top to the bottom of the panel (Fig. 1). The axial struts follow a hysteresis-based model, while the shear strut is characterized by a bilinear force-deformation relationship. Among existing macro models, this approach is considered one of the most comprehensive for representing masonry infills. However, its practical implementation requires defining numerous parameters that are challenging to determine, including Tensile Strength (f'_t), Compressive Strength (f_n), Elastic Modulus (E_{mo}), Closing Strain (ε_{cl}), Strain at Maximum Stress (ε_m), Ultimate Strain (ε_u), Strain Inflection Factor (α_{ch}), Unloading Stiffness Factor (γ_{un}), Reloading Strain Factor (α_{re}), Stress Inflection Factor (β_{ch}), Complete Unloading Strain Factor (β_a), Zero Stress Stiffness Factor (γ_{plu}), Plastic Unloading Stiffness Factor (e_{x1}), Reloading Stiffness Factor (γ_{plr}), Repeated Cycle Strain Factor (e_{x2}), Friction Coefficient (μ), Shear Fraction (γ_s), Bond Shear Strength (τ_o), and Reduction Shear Factor (α_s). For calibration, experimental results from tests conducted on full-scale ductile RC frames infilled with fly ash bricks (230x110x75 mm) were chosen [8,22] for their significantly lower strength and stiffness compared to the RC frame. The motivation behind this choice was to assess the effectiveness of Eurocode 8 design provisions in borderline cases where the amplification of seismic action effects due to masonry infills is minimal or not required. The selected tests referred to as DFS in [22], featured infills constructed with a 1:4 cement-sand mortar mix and a water-cement ratio of 0.6. The masonry walls were laid in a stretcher bond (running bond) pattern. The calibration process was performed using SeismoStruct software [23]. Parameters controlling the hysteresis loop shape (γ_{un}, α_{ch}, and e_{x1}) were adjusted within the ranges specified by Crisafulli [20] to align the numerical response with experimental results [8]. Finally, less influential parameters were modified to minimize discrepancies in pinching effects and strength degradation. The final set of calibrated parameter values is listed in Tab.1.

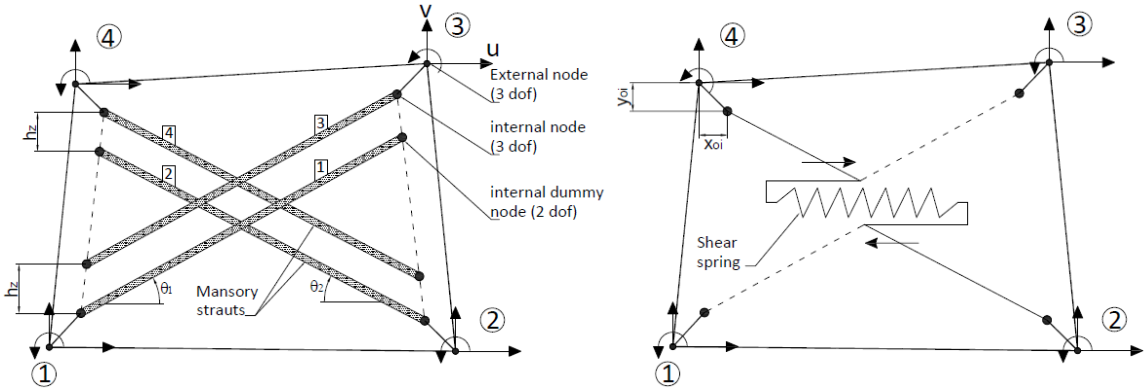

Figure 1: Masonry infill panel model.

Tensile Strength f'_t (kN)	0.5	Reloading strain factor α_{re}	0.48	Shear fraction γ_s (kN)	140
Compressive Strength f_n (kN)	680	Complete unloading strain factor β_a	0.99	Repeated cycle strain factor e_{x2}	1.7
Elastic modulus E_{mo} (kPa)	1158000	Strain inflection factor α_{ch}	0.90	Plastic unloading stiffness factor e_{x1}	3.2
Closing strain ε_{cl}	0.04	Stress inflection factor β_{ch}	1.4	Friction Coefficient μ	0.9
Strain at max stress ε_m	0.004	Zero stress stiffness factor γ_{plu}	0.7	Bond shear strength τ_o (kN)	250
Unloading stiffness factor γ_{un}	1.6	Reloading stiffness factor γ_{plr}	1.7	Reduction shear factor α_s	1.8

Table 1: Model Parameters.

4 PARAMETRIC ANALYSIS

4.1 Hysteretic Model Calibration

The study analyzed a three-story reinforced concrete (RC) frame building with a regular layout. Figs. 2a and 2b show the floor plan and 3D model. The first story is 3.5 meters high, while the upper floors are each 3.0 meters. The bays span 5.00 meters in both directions, with uniformly 20 cm thick slabs. The structure uses B450C steel reinforcement with a tensile strength of 450 MPa. Columns have cross-sections of 40×40 cm, and beams are 40×50 cm. The concrete has a nominal compressive strength of 25 N/mm² (C25/30 class) and a unit weight of 24.0 kN/m³. Designed according to EC8, the building is classified under site class A and Ductility Class Medium (DCM), with a behavior factor (q) of 3.9 for ultimate limit state verifications. The seismic design considered a damping ratio of 5% and a design Peak Ground Acceleration (PGA) of 0.25g at the Life-Safety Limit State. The base shear was calculated as 16% of the building's total seismic weight (W) using the response-spectrum mode superposition method. Since Eurocode 8 does not mandate additional requirements for masonry-infilled frames in medium-ductility structures, these provisions were not applied. The code assumes that lower-ductility RC buildings possess sufficient lateral strength to compensate for infill wall effects, making this study particularly relevant for cases where such additional measures are not required. Capacity design principles were implemented to ensure a proper resistance hierarchy, resulting in a high longitudinal reinforcement ratio for columns ($\rho_l > 2\%$). The column reinforcement consists of 16ϕ18 bars for corner columns and 18ϕ18 bars for the others. Stirrups of 8 mm diameter are placed at 10 cm intervals. The beams are reinforced with 4ϕ14 bars at both the top and bottom and transverse stirrups of 8 mm diameter spaced at 15 cm. For numerical modeling, the following material properties were used: concrete with an elastic modulus of 31,476 MPa, zero tensile strength, and a peak strain of 0.002. The reinforcing steel had an elastic modulus of 210,000 MPa, a strain hardening parameter of 0.005, a fracture/buckling strain of 0.1, and a specific weight of 78 kN/m³. The structural members were modeled in SeismoStruct using inelastic force-based fiber elements (infrmFB).

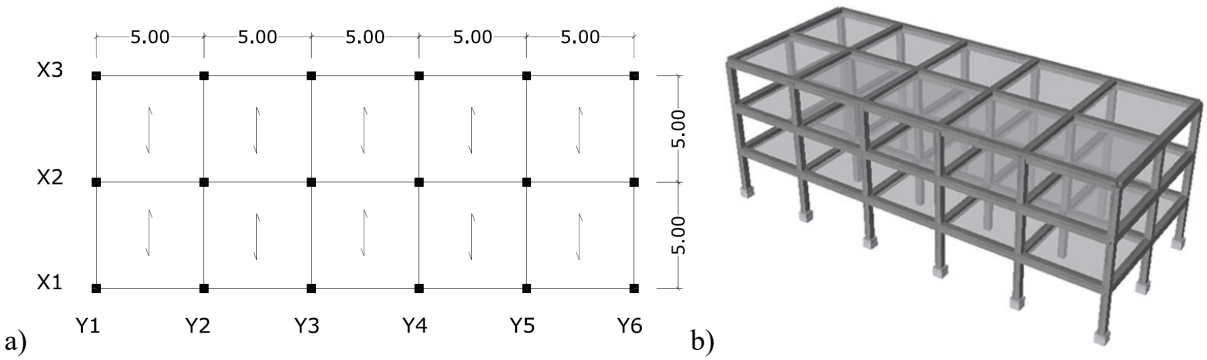

Figure 2: Masonry infill panel model.

4.2 Layouts of infill walls

Reinforced concrete (RC) structures can feature various configurations of masonry infills, which significantly influence their seismic behavior. To assess this impact, different layouts of infill walls were examined. Six case studies (from A to F) with varying configurations, both regular and irregular in plan and elevation, were considered (Figure 3). Irregular distribution of masonry infills can alter the building's seismic response compared to initial design expectations. Asymmetry in infill placement (e.g., Cases B and D) increases eccentricity

between the center of mass and center of stiffness, leading to additional torsional effects. Vertical irregularities (e.g., Cases C, D, E, and F) may create weak-story mechanisms, increasing the risk of collapse in floors lacking infills. Some configurations studied may not fully represent real buildings but were chosen to analyze borderline cases where Eurocode 8 does not require action effect amplifications or additional retrofitting measures. To evaluate the seismic behavior of these structures, two modeling approaches were adopted: 1) Infilled Frame Model: Explicitly incorporates masonry infills using the macro-model described in Section 3.2.; 2) Bare Frame Model: Neglects infill stiffness and strength while applying Eurocode 8 provisions for infilled frames.

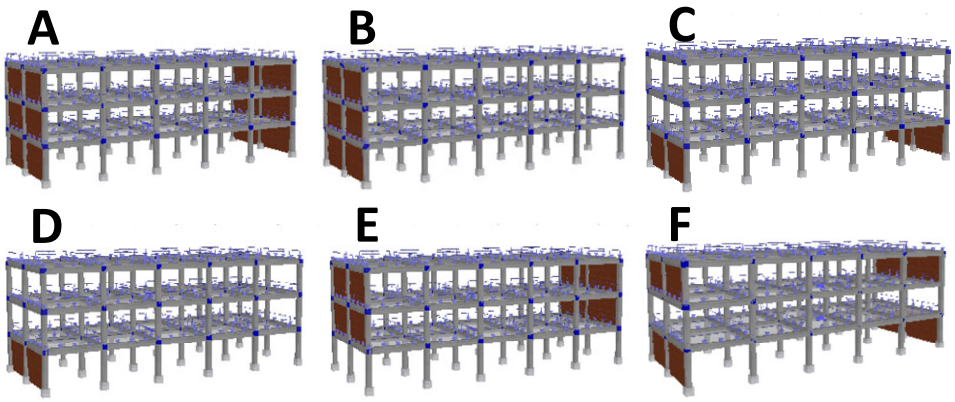

Figure 3: Configurations of masonry infill panels.

4.3 Analyses and Results

The seismic assessment involved both nonlinear static and dynamic analyses. Nonlinear Static Procedures (NSPs) are widely used [24-30] to estimate deformation demands with lower computational complexity than Nonlinear Response History Analysis (NRHA). For this study, nonlinear static (pushover) analyses were conducted per Eurocode 8 [10], applying two lateral load distributions: uniform pattern and first-mode pattern. The relationship between base shear and control displacement (capacity curve) was determined following EC8 provisions [10]. Target displacement was calculated using the N2 method [24], which approximates the capacity curve as an elasto-plastic system and employs the R_μ–μ–T relation from Vidic *et al.* [31] to derive the Inelastic Demand Response Spectrum (IDRS). While extensions of the N2 method for infilled RC frames typically require multi-linear pushover curve idealization and specific R_μ–μ–T relations, this study did not observe significant strength degradation in pushover curves. Therefore, the standard N2 method was used to estimate the Peak Ground Acceleration (PGA_{LS}) at the Life Safety (LS) Limit State. Given the known target displacement, effective period (T), ductility (μ), and reduction factor $R_\mu(T,\mu)$, the N2 method provides an estimate of the elastic spectral acceleration leading to the LS Limit State. The comparison between demand and capacity in Acceleration-Displacement Response Spectrum (ADRS) format is presented in Figs.4-5 for the Infill Frame Model across different case studies (A-F) and lateral load distributions (first mode and uniform). Fig.6 displays the corresponding results for the Bare Frame Model. It is important to note that the masonry walls analyzed exhibit relatively low resistance. Consequently, the magnification factor (K_{IR}), calculated using Eq.1, remains below 1.1, meaning that seismic action effects are not amplified, even in cases with elevation irregularities (C, D, E, and F). However, as per Eurocode 8 [10], irregular infill distribution in plan (e.g., cases B and D) requires an increase in accidental eccentricity by a factor of 2.0.

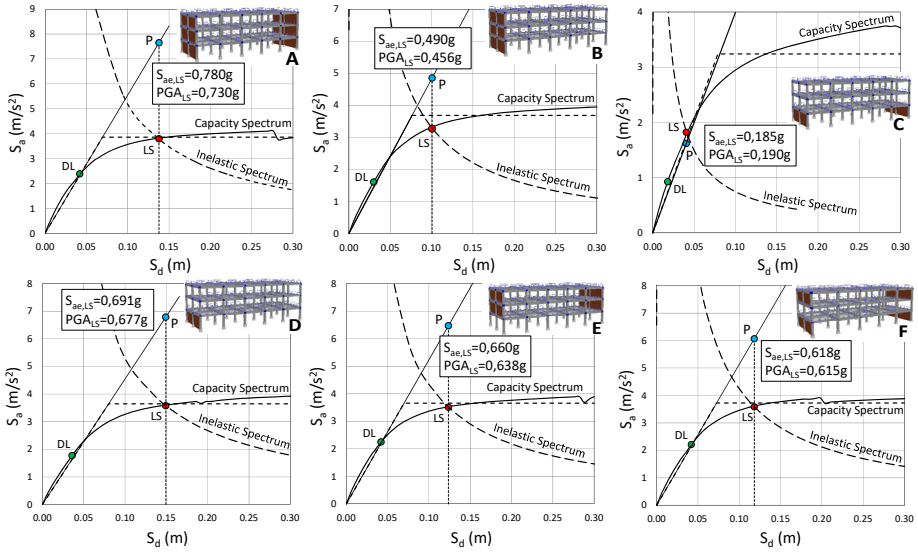

Figure 4: Intersection between demand and capacity - Infilled frames – Uniform Load Pattern.

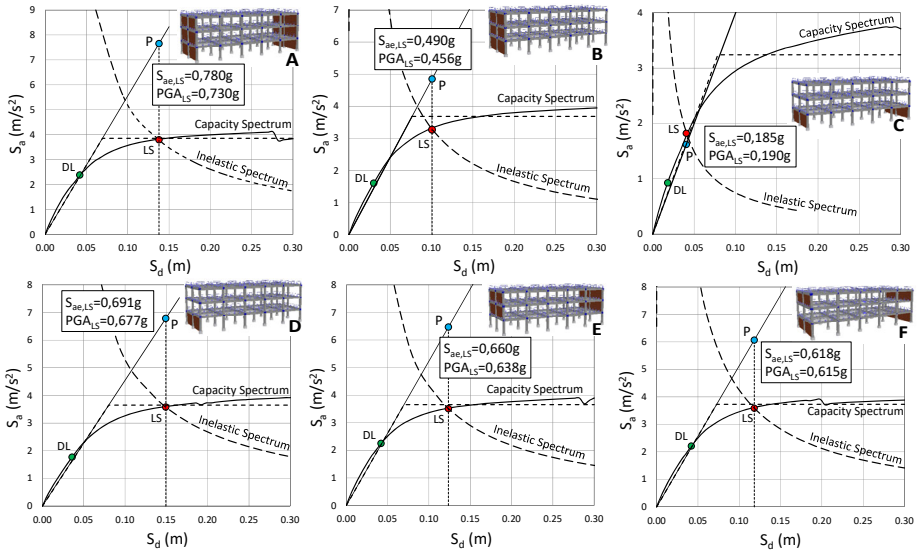

Figure 5: Intersection between demand and capacity - Infilled frames – First-Mode Load Pattern.

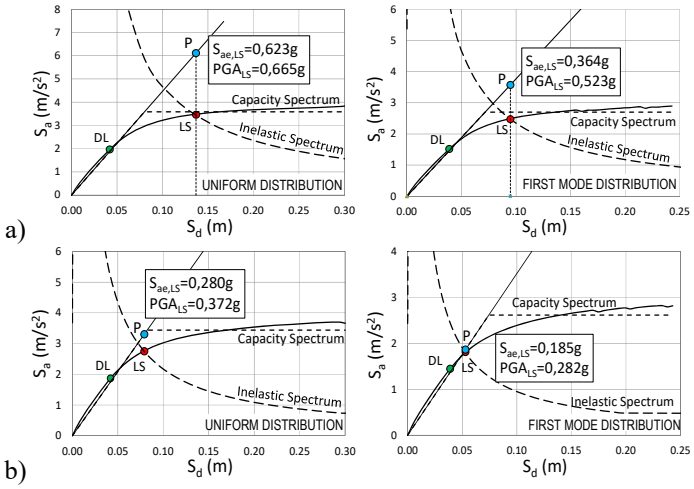

Figure 6: Intersection between demand and capacity – Bare Frame Model.
a) 5% accidental eccentricity; b) 10% accidental eccentricity

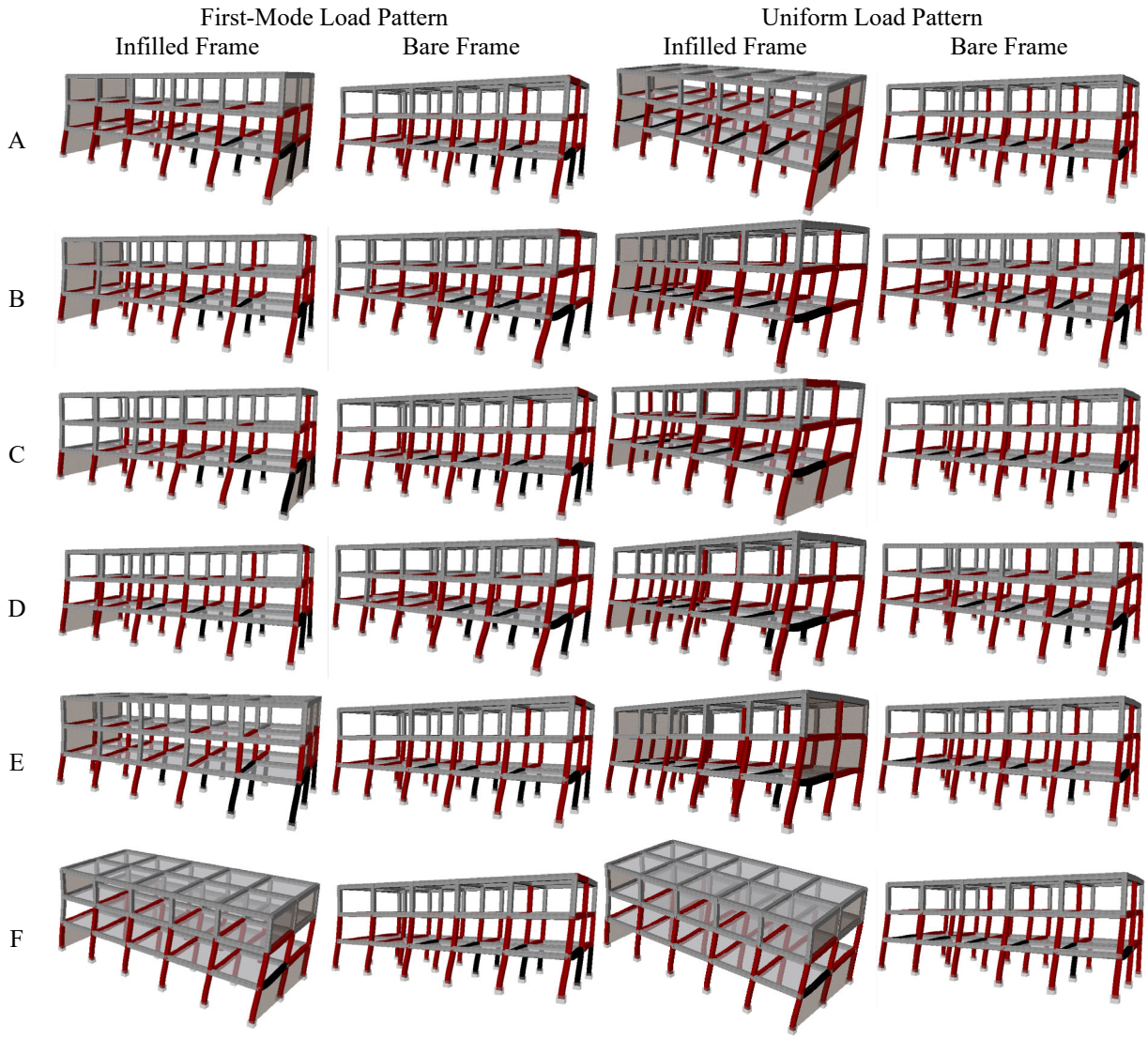

Figure 7: Patterns of yielding (Life Safety Limit State).

Fig. 6 presents results incorporating 5% and 10% accidental eccentricity, derived from pushover analysis in the Y-direction. Key performance points include the Damage Limitation (DL) and Life Safety (LS) Limit States. The DL Limit State is determined by chord rotation at yielding (θ_y) using EN 1998-3 formulas [32], while the LS Limit State is defined as 3/4 of the ultimate chord rotation (θ_u). Pushover curves (Figs. 4-5) indicate no strength degradation before reaching the LS Limit State, attributed to the use of fly ash brick infills, which are more deformable than the RC frame and have a drift capacity of around 2% before significant degradation. Table 2 compares results between the Infill Frame Model and the Bare Frame Model with Eurocode 8 provisions. Regular structures (Case A) require no additional provisions, while cases with elevation irregularities (C, E, F) have stiffness ratios ($K_{IR} < 1.1$) that do not necessitate amplification, using 5% eccentricity results. Cases with plan irregularities (B, D) require an increased accidental eccentricity factor of 2.0 (10%), with results based on the Bare Frame Model (Fig. 6b). Fig. 7 illustrates yielding patterns at the LS Limit State, showing that cases A, E, and F exhibit similar behavior in both models. However, cases B and D display torsional effects due to irregular infill distribution, concentrating deformations on the flexible side without infill panels. This behavior is also observed in the Bare Frame Model when EC8 provisions are applied with 10% eccentricity, confirming their conservatism for plan-irregular

structures. Case C demonstrates a unique response under uniform lateral loading. Increased accidental eccentricity induces torsional rotation, amplifying stress in infill panels of Frame Y6. Due to the brittle nature of masonry, Frame Y6 experiences a sharp strength reduction, shifting inelastic demands to the flexible side, leading to premature masonry failure. This extreme behavior does not appear in the Bare Frame Model or the Infill Frame Model under the first mode distribution. Consequently, PGA_{LS} for the Infill Frame Model under uniform loading is significantly lower (0.190g) than for the first mode (0.520g) and the Bare Frame Model (0.665g) (Tab.2). These findings highlight that in some cases, masonry infills cannot be ignored in structural models, as they critically influence failure mechanisms. Neglecting them may lead to unsafe design assumptions.

The shear demand on the columns of infilled frames was analyzed to understand its impact. The total shear demand in a column ($V_{D,t}$) was computed as the sum of the shear force from the analysis ($V_{D,a}$) and the additional shear force induced by the masonry infill ($V_{D,i}$), calculated as follows: $V_{D,i}= \gamma_{ci} \cdot N_s \cdot \cos(\theta)$, where N_s represents the axial force in the equivalent diagonal strut, θ is its inclination, and γ_{ci} indicates the fraction of the force transferred from the infill to the column. Celarec *et al.* [33] found that γ_{ci} depends on the ratio of column stiffness to infill stiffness, varying from 0.44 to 0.58 based on the column's location in the building. In this study, γ_{ci} was set at 0.5, ignoring the effect of column location, as the column-to-infill stiffness ratio was high due to the use of fly ash bricks. Fig. 8 illustrates the shear demand in the first-story corner column of Frame Y1 (case study C) during pushover analysis under uniformly distributed lateral loads. Diagonal failures in compression occur before LS Limit State when the column's shear force is still increasing with displacement, indicating that the effect of the masonry infill on shear demand is minimal. Additionally, the total shear demand remains well below the estimated shear strength from Eurocode 8. Fig. 8 compares the total shear demand of the corner column at the displacement corresponding to the LS performance level with the results from the Bare Frame Model, which includes additional EC8 measures for infilled frames. In the case study D, the shear demand in the Infilled Frame Model exceeds that of the Bare Frame Model, with an increase of up to 30% at the upper story. This increase depends on the variation in the nonlinear static response of the RC frame due to the infill panels. As a result, the Bare Frame Model is not conservative for case study D, even when Eurocode provisions are applied to mitigate the potential effects of infill irregularity in plan.

Finally, the impact of masonry infills on the inelastic dynamic response of the buildings was assessed using seven accelerograms from European databases [34]. The accelerograms met the seismic standards and were scaled to a 0.25 g acceleration. Accidental eccentricity effects were considered, with a 5% shift in the center of mass and an increased 10% eccentricity for irregular infill distributions, as per EC8 provisions. Fig. 9 shows the mean of Y-top lateral displacements from nonlinear response-history analysis. The results indicate that the Bare Frame Model provides conservative estimates if EC8 provisions are applied.

Case Study	Uniform Distribution		First Mode Distribution	
	Infill Frame Model	Bare Frame Model + EC8 measures	Infill Frame Model	Bare Frame Model + EC8 measures
A	0.730	0.665	0.532	0.523
B	0.456	0.372	0.338	0.282
C	0.190	0.665	0.520	0.523
D	0.677	0.372	0.408	0.282
E	0.638	0.665	0.540	0.523
F	0.615	0.665	0.528	0.523

Table 2: Capacity peak ground acceleration (PGA_{LS}) at Life Safety (LS) Limit State.

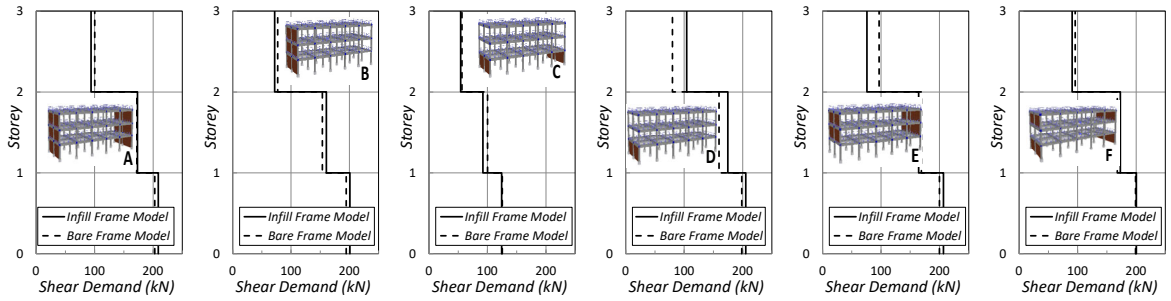

Figure 8: Distribution of shear demand over the height.

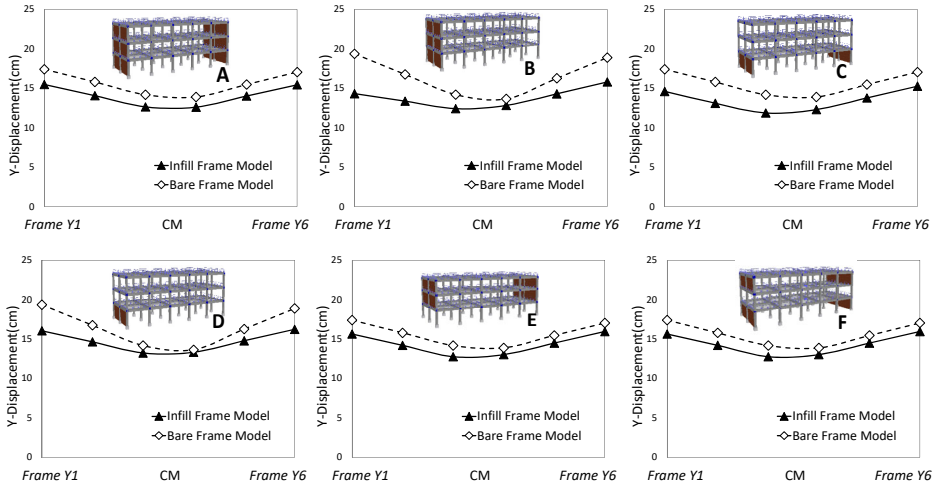

Figure 9: Mean Y-top lateral displacements from nonlinear response history analysis.

5 CONCLUSIONS

Masonry infills significantly affect the building's inelastic response, even with regular distribution or when Eurocode 8 provisions for irregular infill distribution are applied. Structural failures such as torsion and soft-story effects are highlighted. In cases with regular plan distribution but irregular elevation, accidental eccentricity causes torsional rotation, increasing stresses on one side's infill panels. These panels lose strength, increasing frame member stresses and triggering torsion and soft-story effects. The inelastic behavior seen in the infilled frame model does not occur in the bare frame model, which shows higher peak ground acceleration capacity. This suggests that neglecting infill panels' contribution is not conservative, even with Eurocode 8 provisions. Applying Eurocode 8 provisions can significantly increase shear demand on columns due to local frame-infill interaction and nonlinear response variation. If columns are not designed for seismic conditions, this could lead to brittle shear failure and unexpected non-ductile collapse mechanisms. The study neglects out-of-plane failure of infills, considers only infills without openings, and does not explicitly model potential column shear failures, though shear demand is checked against capacity. Eurocode 8 provisions for irregularities in infill distribution are included in the analysis.

REFERENCES

[1] A. Furtado, H. Rodrigues, A. Arede, Modelling of masonry infill walls participation in the seismic behaviour of RC buildings using OpenSees. *Int. J. Adv. Struct.* (IJASE), **7**, Issue 2, 117–127, 2015.

[2] M. Dolsek, P. Fajfar, Mathematical modelling of an infilled RC frame structure based on the results of pseudo-dynamic tests. *Earthq. Eng. Struct. Dyn.*, **31**, 1215–1230, 2002.

[3] M. Ferraioli, Case study of seismic performance assessment of irregular RC buildings: hospital structure of Avezzano (L'Aquila, Italy). *Earthq. Eng. Eng. Vib.*, **14**, 141-156, 2015.

[4] M. Ferraioli, O. Pecorari, D. Farace, G. Di Lauro, Influence of torsional effects in seismic retrofit of RC buildings. *Procedia Struct. Integr.*, **64**, 1017–1024, 2024.

[5] M. Dolsek, P. Fajfar, The effect of masonry infills on the seismic response of a four storey reinforced concrete frame - a probabilistic assessment, *Eng. Struct.*, **30**, 3186–92, 2008.

[6] Y.P. Yuen, J.S. Kuang, Nonlinear seismic response and lateral force transfer mechanisms of RC frames with different infill configurations, *Eng. Struct.*, **91**, 125–40, 2015.

[7] G. Mondal, S. Tesfamariam, Effects of vertical irregularity and thickness of unreinforced masonry infill on the robustness of RC framed buildings, *Earthq. Eng. Struct. Dyn.*, **43**, 205–23, 2014.

[8] M. Ferraioli, A. Lavino, Irregularity Effects of Masonry Infills on Nonlinear Seismic Behaviour of RC Buildings. *Math. Probl. Eng.*, 4086320, 2020.

[9] A.F. Mohammad, M. Faggella, R. Gigliotti, E. Spacone, Seismic performance of older R/C frame structures accounting for infills-induced shear failure of columns, *Eng. Struct.*, **122**, 1-13, 2016.

[10] CEN European standard EN1998-1, *Eurocode 8: design of structures for earthquake resistance, Part 1: general rules, seismic action and rules for buildings*, European Committee for Standardisation, Brussels, 2004.

[11] M.N. Fardis, Design provisions for masonry-infilled RC frames, *Proc. 12th World Conference on Earthquake Engineering*, Auckland, Paper No. 2553, 2000.

[12] NTC-2018 Guidelines, *Technical Standards for Constructions*, Official Journal of the Italian Republic, 20.02.2018, Rome, Italy, 2018, (in Italian).

[13] NTC-Instruction 2019, *Instructions for the application of the new technical norms on constructions* (in Italian), Official Journal of the Italian Republic, Circ. 21.01.2019, n.7, 2019, (in Italian).

[14] Federal Emergency Management Agency (FEMA), *Prestandard and Commentary for the Seismic Rehabilitation of Buildings*, FEMA 356, Washington, DC, USA, 2000.

[15] R.J. Mainstone, *Supplementary note on the stiffness and strength of infilled frames*, Current paper CP13/74 London (UK): Building Research Establishment, 1974.

[16] Federal Emergency Management Agency (FEMA), *NEHRP commentary on the guidelines for the seismic rehabilitation of buildings*, FEMA-274, Washington, DC, USA, 1997.

[17] Federal Emergency Management Agency (FEMA), *Evaluation of earthquake damaged concrete and masonry wall buildings: basic procedures manual*, FEMA-306, Washington, DC, 1998.

[18] P.G. Asteris, D.M. Cotsovos, C.Z. Chrysostomou, A. Mohebkhah, G.K. Al-Chaar, Mathematical micromodelling of infilled frames: state of art, *Eng. Struct.*, **56**, 1905–21, 2013.

[19] F.J. Crisafulli, A.J. Carr, R. Park, Analytical modelling of infilled frames structures – a general review. *Bull. N. Z. Soc. Earthq. Eng.*, **33**(1), 30–47, 2000.

[20] F.J. Crisafulli, A.J. Carr, Proposed macro-model for the analysis of infilled frame structures. *Bull. N. Z. Soc. Earthq. Eng.*, vol. 40(2), pp. 69-77, 2007.

[21] L. Cavaleri, F. Di Trapani, Cyclic response of masonry infilled RC frames: experimental results and simplified modelling. *Soil Dyn. Earthq. Eng.*, **65**, 224–42, 2014.

[22] S.H. Basha, H.B. Kaushik, Behavior and failure mechanisms of masonry-infilled RC frames (in low-rise buildings) subject to lateral loading. *Eng. Struct.*, **111**, 233–245, 2016.

[23] SeismoStruct: *A computer program for static and dynamic analysis for framed structures*, SeismoSoft, [Online] Available from URL: www.seismosoft.com, 2023.

[24] P. Fajfar, A Nonlinear Analysis Method for Performance Based Seismic Design. *Eartq. Spectra,* **16**(3), 573-592, 2000.

[25] M. Dolsek, P. Fajfar, Simplified non-linear seismic analysis of infilled reinforced concrete frames. *Earthq. Eng. Struct. Dyn.*, **34**, 49–66, 2005.

[26] M. Ferraioli, A. Lavino, A. Mandara, An adaptive capacity spectrum method for estimating seismic response of steel moment-resisting frames. *Ingegneria Sismica*, **33**(1-2), 47-60, 2016.

[27] A.K. Chopra, R.K. Goel, A modal pushover analysis procedure for estimating seismic demands for buildings. *Earthq. Eng. Struct. Dyn.*, **31**(3), 561–582, 2002.

[28] H. Sucuoğlu, M.S. Günay, Generalized force vectors for multi-mode pushover analysis. *Earthq. Eng. Struct. Dyn.*, **40**, 55–74, 2011.

[29] M. Ferraioli, Multi-mode pushover procedure for deformation demand estimates of steel moment-resisting frames. *Int. J. Steel Struct.*, **17**(2), 653-676, 2017.

[30] M. Ferraioli, A. Lavino, A. Mandara, Effectiveness of multi-mode pushover analysis procedure for the estimation of seismic demands of steel moment frames. Ingegneria Sismica, **35**(2), 78-90, 2018.

[31] T. Vidic, P. Fajfar, M. Fischinger, Consistent Inelastic Design Spectra: Strength and Displacement. *Earthq. Eng. Struct. Dyn.*, **23**, 502–521, 1994.

[32] CEN European standard EN1998-3, *Eurocode 8 - Design of structures for earthquake resistance - Part 3: Assessment and retrofitting of buildings*, European Committee for Normalization, Brussels, 2005.

[33] D. Celarec, M. Dolsek, Practice-oriented probabilistic seismic performance assessment of infilled frames with consideration of shear failure of columns. *Earthq. Eng. Struct. Dyn.*, **42**(9), 1339-1360, 2013.

[34] I. Iervolino, C. Galasso, E. Cosenza, REXEL: computer aided record selection for code-based seismic structural analysis, *Bull. Earthq. Eng.*, **8**, 339-362, 2010.